Clays and Clay Minerals, Vol. 53, No. 4, 372–379, 2005.

REACTION OF PHOSPHATE COMPOUNDS WITH A HIGH-SILICA ALLOPHANE

KIYOSHI OKADA[1,*], KOJI NISHIMUTA[1], YOSHIKAZU KAMESHIMA[1], AKIRA NAKAJIMA[1] AND KENNETH J. D. MACKENZIE[2]

[1]Department of Metallurgy and Ceramics Science, Graduate School of Science and Engineering, Tokyo Institute of Technology, O-okayama, Meguro, Tokyo 152-8552, Japan

[2]School of Chemical and Physical Sciences, Victoria University of Wellington, P.O. Box 600 Wellington, New Zealand

Abstract—The loading of various phosphates on the surfaces of nanoparticles of allophane ($1-2SiO_2 \cdot Al_2O_3 \cdot 5-6H_2O$) was investigated. The allophane used was a high-silica type with a Si/Al ratio of 0.85. The phosphate-sorption isotherm was measured using $(NH_4)_2HPO_4$ solution, which showed the highest phosphate sorption of the seven phosphates examined. This sorption isotherm was in better agreement with the Langmuir equation than the Freundlich equation. The resulting maximum sorption capacity was 4.87 mmol/g and the Langmuir constant was 0.0033 L/mmol. The sorption energy (ΔG) calculated from the Langmuir constant was −2.96 kJ/mol. The amount of loaded phosphate varied greatly according to the phosphate used, being greater for orthophosphates than for polyphosphates. The amount of loaded phosphate also depended on the cation present, in the order Ca-Na-NH_4-phosphate. The Si/Al ratios of the samples were decreased by orthophosphate loading due to the partial replacement of SiO_4 by PO_4 tetrahedra, but this effect was offset by the partial dissolution of the allophane by polyphosphate loading. The ^{29}Si magic angle spinning nuclear magnetic resonance (MAS NMR) spectra of all the phosphate-loaded samples showed an increase of a peak at −90 ppm (the Q^1-Q^3 polymerized tetrahedral unit) and the decrease of a peak at −78 ppm peak (the Q^o monomeric tetrahedral unit). The ^{31}P MAS NMR spectra showed peaks at ~−10 ppm, assigned to Q^2 units corresponding to polymerized tetrahedra which consisted of loaded PO_4 together with $Si(Al)O_4$. The structure changes produced in allophane by phosphate loading are discussed in light of these data.

Key Words—Allophane, Phosphate-loading, Sorption Properties, Structure Change.

INTRODUCTION

Allophane is a mineral widely distributed in weathered volcanic ash soil, showing a unique structure consisting of hollow spherical particles 3.5−5 nm in diameter (Kitagawa, 1971). Since allophane is an X-ray amorphous substance, its structure has not yet been clearly elucidated. The many proposed structure models fall into two groups, a kaolinite-like model (Okada *et al*., 1975; MacKenzie *et al*., 1991; Lindner *et al*., 1998) and an imogolite-like model (Parfitt *et al*., 1980; Padilla *et al*., 2002a). However, the two models postulate structural defects in both the octahedral and tetrahedral sheets, which allow small molecules such as H_2O access to the interior of the hollow particles. Wada (1979) suggested that charge balance is achieved in allophane by these structure defects, with the presence of tetrahedral Al yielding Brønsted acid sites. Allophane is known to show both positive and negative surface charges at about neutral pH due to these structure defects. Thus, allophane has the unique property of relatively large cation exchange capacity (CEC) and anion exchange capacity (AEC) at about neutral pH.

Because of the unique CEC and AEC properties of allophane, many studies have been reported on its adsorption of various ions, especially oxyanions such as phosphate (Johan *et al*., 1997), sulfate (Padilla *et al*., 2002a), silicate (Nartey *et al*., 2001), molybdate (Elhadi *et al*., 2000), borate (Son *et al*., 1998), nitrate (Padilla *et al*., 2002b), *etc*. As a general trend, the amount of sorption increases with increasing Si/Al ratio of the allophane, corresponding to the AEC value. The maximum sorption capacity of allophane is reported to be of the order of several hundred μmol/g for polyvalent anions but less than this for monovalent anions. Sorption of these oxyanions causes increased cation retention and the release of silicate ions from the allophane (Nanzyo, 1995). The sorption sites of these anions in allophane are thought to be the $Al(O,OH)_6$ octahedra, especially the defects at these sites.

Sorption studies of phosphate by allophane have been driven mainly by their importance to agriculture (phosphate is an important fertilizer for various crops). In addition, Tarasevich and Klimova (2001) found a distinct enhancement in the uptake of heavy metal ions by kaolinite and Al oxide when their surfaces were modified by phosphate sorption. This remarkable enhancement appears to be caused by the surface phosphate loaded on to Al−OH bonds, though the mechanism is not discussed in the paper. This result is thought to be related to the efficient uptake of various heavy metal ions shown by $AlPO_4$ (Naeem *et al*., 2002). As the surface area of kaolinite is not sufficiently high for it to act as an efficient host material for phosphate

* E-mail address of corresponding author:
kokada@ceram.titech.ac.jp
DOI: 10.1346/CCMN.2005.0530405

loading, this effect should be further enhanced in compounds with greater surface area. Allophane is therefore a candidate material for phosphate loading. The effect of phosphate loading on the uptake of Cu^{2+} has been investigated using natural and synthetic allophanes with low Si/Al ratios (Clark and McBride, 1985). The Cu^{2+} uptake is found to increase with increasing content of phosphate loaded on the allophanes. However, the maximum amount of phosphate sorption achieved by these authors was ~0.5 mmol/g because their allophanes were of relatively low Si/Al ratio, giving them a low phosphate-sorption capacity (Johan *et al*., 1997).

It is therefore interesting to examine the effect of phosphate loading on the uptake of heavy metal ions by allophanes of higher Si/Al ratio with a greater loading capacity for phosphate. In this paper, allophane with high Si/Al ratio was loaded with various phosphates to determine the effect of the phosphate type on the amount of phosphate sorption.

EXPERIMENTAL METHOD

Preparation

Allophane was collected from Kanuma pumice bed, Kanuma, Tochigi, Japan and purified by elutriation (2 μm) using a Na hexametaphosphate dispersant. The elutriated sample was dried at 60ºC overnight in an oven.

The phosphate sorption isotherm of allophane was determined to elucidate the initial phosphate concentration necessary for loading a saturated amount of phosphate on to the allophane. The sorption experiments were performed using solutions containing various concentrations of $(NH_4)_2HPO_4$, the pH being adjusted to 4 with HCl at 25ºC, and stirred for 24 h.

Phosphate-loading experiments were then performed using solutions containing various phosphates with the pH adjusted to 4. The phosphates used in these experiments were: three orthophosphates ($(NH_4)_2HPO_4$, Na_2HPO_4, $CaHPO_4{\cdot}2H_2O$), pyrophosphate ($Na_4P_2O_7{\cdot}10H_2O$), triphosphate ($Na_5P_3O_{10}$), hexametaphosphate ($Na_6(PO_3)_6$) and polyphosphate ($Na_{2n-1}P_nO_{3n-1}$). The concentrations of these phosphates were set to 0.8 M except for the less soluble $CaHPO_4{\cdot}2H_2O$ (0.04 M) and $Na_4P_2O_7{\cdot}10H_2O$ (0.25 M). These concentrations are considered to be sufficiently high for saturated sorption of phosphate to occur. Allophane (1 g) was dispersed in the solution (100 mL) at 25ºC and reacted for 24 h with stirring. The phosphate-loaded samples were washed three times with distilled water, centrifuged and dried at 60ºC overnight.

Characterization

X-ray diffraction (XRD) patterns were recorded on a diffractometer (XRD6100, Shimadzu) with monochromated CuKα radiation. The bulk chemical compositions of the allophane with and without phosphate loading were determined by X-ray fluorescence (XRF) using a Rigaku RIX2000 spectrometer. Their surface compositions were measured by X-ray photoelectron spectroscopy (XPS) using a Perkin Elmer Model 5500MT spectrometer with MgKα radiation. The amount of phosphate sorption was calculated from the difference of the concentrations before and after sorption using an ICP spectrometer (Prodigy, JEOL). The differential thermal analysis/thermogravimetric (DTA/TG) curves were recorded up to 1300ºC at a heating rate of 10ºC/min with a sample weight of ~15 mg (Thermoplus TG8120, Rigaku). The Fourier transform infrared (FTIR) spectra were measured by the diffuse reflectance method using an FTIR spectrometer (FTIR 8200PC, Shimadzu). Solid-state ^{29}Si, ^{27}Al and ^{31}P MAS NMR spectra were obtained at 11.7 T using a Varian Unity 500 spectrometer and Doty probe spun at 10−12 kHz. The ^{29}Si spectra were acquired using a 90º pulse of 60 μs and a recycle delay time of 100 s, and were referenced to tetramethylsilane (TMS). The ^{27}Al spectra were acquired using a 15º pulse of 1 μs and a recycle delay time of 1 s and were referenced to $Al(H_2O)_6^{3+}$. The ^{31}P spectra were determined at a spectrometer frequency of 202.331 MHz using a 60º pulse of 3 μs and a recycle delay time of 1 s and were referenced to 85% H_3PO_4.

RESULTS AND DISCUSSION

Phosphate sorption isotherm

The measured phosphate sorption isotherm data were fitted by the least-squares method using Langmuir (1) and Freundlich (2) equations shown below:

$$Q_e = Q_0 b C_e/(1+bC_e) \quad (1)$$

$$Q_e = K C_e^{1/n} \quad (2)$$

where Q_e (mmol/g) and C_e (mmol/L) are the equilibrium phosphate adsorption and concentration, Q_0 (mmol/g) is the maximum monolayer adsorption capacity, b is the Langmuir constant (L/mmol), and K (mmol/g) and n are the Freundlich constants. The correlation coefficient (r) obtained from the calculation using Langmuir equation is $r = 0.995$, better than when the Freundlich equation is used. The observed data and the curve calculated using the experimental Langmuir parameters are shown in Figure 1. The resulting Q_0 and b values are 4.87 mmol/g and 0.0033 L/mmol, respectively. The sorption energy (ΔG) was determined from the equation $\Delta G = -RT\ln(b)$ to be −2.97 kJ/mol. Since this value is negative, the sorption occurs spontaneously. The absolute value of the phosphate sorption energy in this sample is very small and rather similar to the values for physical sorption (several kJ/mol). Setting the initial concentration of phosphate for the loading experiments to $\geqslant$0.4 M is found to be sufficient.

The resulting Q_0 value is much higher than reported elsewhere (0.4−1.8 mmol/g; Rajan, 1975). The phos-

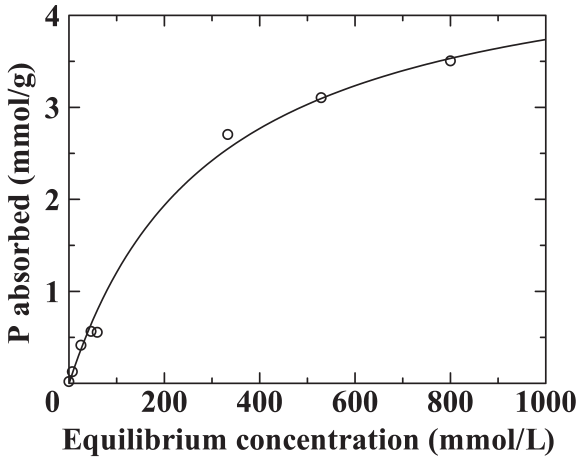

Figure 1. Phosphate-sorption isotherm obtained using $(NH_4)_2HPO_4$ solution. The curve in the figure is based on experimental Langmuir parameters.

phate is thus thought to be sorbed not only by adsorption but also by other mechanisms such as precipitation. In phosphate sorption on allophane and aluminosilicate gels, two sorption mechanisms are generally considered (Rajan, 1975; Nanzyo, 1987). Rajan (1975) proposed the sorption mechanisms of ion substitution (ligand exchange) at lower initial phosphate concentrations and precipitation at higher concentrations, based on the two different slopes in the Freundlich plot of their experimental data. By contrast, our data showed no discontinuity and could be fitted by one straight line in the Langmuir plot. Although our experimental data are compatible with a single sorption mechanism rather than two sorption mechanisms, two sorption mechanisms such as ion substitution and precipitation could plausibly explain the present high Q_0 value.

PO_4 loading by various phosphates

The XRF chemical compositions (wt.%) of the allophanes loaded with various phosphates are listed in Table 1 together with that of the unloaded allophane. These data, re-calculated in atomic %, are listed in Table 2, together with the XPS element analysis of the surface. The amounts of phosphate loaded on the allophane are significantly high but differ with the various phosphate compounds used in the experiments. The amount of loaded P (10−25 atomic % in the orthophosphate-loaded samples) was greater than in the polyphosphate-loaded samples (5−6 atomic %). The greatest amount of phosphate loaded on the $(NH_4)_2HPO_4$-treated sample is calculated from the XRF data to be ~4.06 mmol P/g, in good agreement with the maximum sorption capacity (Q_0 = 4.87) determined from the sorption isotherm. The amount of loaded phosphate in this sample is about eight times greater than in the sample prepared by Clarke and McBride (1985). The phosphate content in the $(NH_4)_2HPO_4$-treated sample corresponds to ~80% of monolayer coverage of the surface of Al octahedral sheet of allophane by PO_4 and SiO_4 tetrahedra, assuming an imogolite-like structure model with sorption on the tetrahedral allophane surface layer. The present results also indicate that phosphate loading influences the Si and Al contents of the samples. The Si/Al ratios measured by XRF and XPS were decreased from 0.8−0.9 in the starting material to 0.7−0.8 by orthophosphate loading but were increased to 0.9−1.2 by polyphosphate loading. Since the solutions after orthophosphate loading contain 3−8 mM of Si^{4+} but not Al^{3+} or Fe^{3+} (Table 3), the phosphate is thought to partially replace the silicate of the allophane in this case. Similar results were reported by Nanzyo (1995) and Nartey *et al.* (2001) for sorption of orthophosphate, suggesting that this is a general trend in orthophosphate sorption. By contrast, the trend observed for polyphosphate loading has not previously been reported. After polyphosphate loading, the solutions contain Al^{3+} and Fe^{3+} as well as Si^{4+} as listed in Table 3. Thus, part of the allophane is dissolved during polyphosphate loading. As the concentrations of Si^{4+} are lower than those of Al^{3+} and Fe^{3+}, if all these species result from the dissolution of allophane, part of the dissolved Si^{4+} must be sorbed on the samples, increasing the Si/Al ratios. In this way, a range of Si/Al ratios results from the loading of orthophosphates and polyphosphates. By contrast, the (Si+P)/Al ratios lie within a narrow range (1.0−1.3), irrespective of the type of loading phosphate. In addition to the loaded phosphate, some of the cations (M) from the loading

Table 1. Chemical compositions (wt.%) of the allophanes with and without grafted phosphates (in dry base).

Sample	SiO_2	Al_2O_3	Fe_2O_3	P_2O_5	TiO_2	CaO	MgO	K_2O	Na_2O	SiO_2/Al_2O_3*
Allophane	45.78	46.02	4.64	1.45	0.54	0.19	0.12	0.09	1.18	1.69
$(NH_4)_2HPO_4$-loaded	30.19	36.43	3.85	28.86	0.55	0.09	0.00	0.05	0.00	1.41
Na_2HPO_4-loaded	32.54	38.37	3.99	20.94	0.51	0.10	0.00	0.05	3.50	1.44
$CaHPO_4$-loaded	37.88	40.63	3.99	11.68	0.69	5.03	0.00	0.09	0.00	1.58
$Na_4P_2O_7$-loaded	47.68	38.51	4.31	7.00	0.49	0.11	0.00	0.00	1.90	2.10
$Na_5P_3O_{10}$-loaded	46.35	39.22	4.38	7.23	0.59	0.08	0.00	0.05	2.10	2.01
$(NaPO_3)_6$-loaded	45.33	41.13	4.33	6.36	0.53	0.05	0.00	0.05	2.22	1.87
$Na_{2n-1}P_nO_{3n-1}$-loaded	46.54	39.63	4.28	6.80	0.67	0.06	0.00	0.06	1.96	2.00

* molar ratio

Table 2. Cation compositions (atomic %) of the samples measured by XRF and XPS (in dry base).

Sample	Method	Si	Al	Fe	P	Ti	Ca	Mg	K	Na	Si/Al	(Si+P)/Al	*M**/P
Allophane	XRF	42.46	50.22	3.24	1.14	0.38	0.18	0.17	0.10	2.11	0.85	0.87	—
	XPS	45.66	49.64	2.25	b.d.	b.d.	b.d.	b.d.	b.d.	2.45	0.92	0.92	—
$(NH_4)_2HPO_4$-loaded	XRF	29.92	42.47	2.87	24.18	0.41	0.09	b.d.	0.06	b.d.	0.70	1.27	—
	XPS	32.88	43.66	1.59	21.87	b.d.	b.d.	b.d.	b.d.	b.d.	0.75	1.25	—
Na_2HPO_4-loaded	XRF	30.78	42.70	2.84	16.75	0.36	0.10	b.d.	0.05	6.42	0.72	1.11	0.38
	XPS	28.54	40.01	1.79	22.32	b.d.	b.d.	b.d.	b.d.	7.35	0.71	1.27	0.33
$CaHPO_4$-loaded	XRF	36.22	45.71	2.87	9.44	0.50	5.16	b.d.	0.11	b.d.	0.79	1.00	0.55
$Na_4P_2O_7$-loaded	XRF	44.86	42.62	3.05	5.57	0.35	0.11	b.d.	b.d.	3.45	1.05	1.18	0.62
	XPS	47.45	41.09	1.85	5.83	b.d.	b.d.	b.d.	b.d.	3.78	1.15	1.30	0.65
$Na_5P_3O_{10}$-loaded	XRF	43.50	43.30	3.09	5.73	0.42	0.08	b.d.	0.06	3.82	1.00	1.14	0.67
	XPS	44.77	43.09	2.27	5.41	b.d.	b.d.	b.d.	b.d.	4.46	1.04	1.16	0.82
$(NaPO_3)_6$-loaded	XRF	42.30	45.16	3.04	5.02	0.37	0.05	b.d.	0.06	4.01	0.94	1.05	0.80
	XPS	44.41	43.54	1.66	6.39	b.d.	b.d.	b.d.	b.d.	4.01	1.02	1.17	0.63
$Na_{2n-1}P_nO_{3n-1}$-loaded	XRF	43.67	43.75	3.02	5.39	0.47	0.06	b.d.	0.07	3.55	1.00	1.12	0.66
	XPS	45.16	43.92	1.72	5.72	b.d.	b.d.	b.d.	b.d.	3.48	1.03	1.16	0.61

* cation in used phosphates
b.d.: below detection limit

Table 3. Concentrations and pH of the solutions after the phosphate-loading experiments.

Sample	pH	Concentration (mM)		
		Si	Al	Fe
$(NH_4)_2HPO_4$-loaded	4.37	8.13	0.00	0.00
Na_2HPO_4-loaded	4.32	7.25	0.00	0.00
$CaHPO_4$-loaded	4.77	2.95	0.00	0.00
$Na_4P_2O_7$-loaded	4.32	12.70	23.20	1.35
$Na_5P_3O_{10}$-loaded	4.13	10.80	18.80	1.10
$(NaPO_3)_6$-loaded	4.87	7.93	13.50	0.30
$Na_{2n-1}P_nO_{3n-1}$-loaded	4.15	9.23	16.90	0.51

compounds are retained in the loaded samples (Table 2) except in the case of $(NH_4)_2HPO_4$. The presence of NH_4^+ is, however, confirmed by the FTIR spectrum. The *M*/P ratio is 0.3−0.4 for Na_2HPO_4 loading but is higher (0.6−0.8) for polyphosphate loading. Since this result is not consistent with the *M*/P ratios of the starting phosphates, retention of the *M* cation is thought to be related to the effective charge of the loaded phosphates, *i.e.* the difference of negative charge between them.

As listed in Table 2, the surface chemical compositions of all the samples, measured by XPS, show no significant difference compared with the bulk chemical compositions measured by XRF. This may mean that the whole of the allophane particle is analyzed in the present XPS measurements because the particle size is comparable with the depth detectable by XPS surface-analysis techniques. This result also suggests that no precipitated phase and/or separated phase is formed on the surface of phosphate-loaded allophane.

The XRD patterns of the samples before and after phosphate loading are shown in Figure 2. No change was observed in any of the phosphate-loaded samples compared to the starting allophane, and in all the samples the loaded phosphates are X-ray amorphous. Although crystalline phases such as taranakite ($H_6K_3Al_5(PO_4)_8{\cdot}18H_2O$; Smith and Brown, 1959) and related compounds are reported to be formed by reaction of allophane with phosphate solution (Wada, 1959), such crystalline phases were not detected in the present samples. This may be due to the difference in reaction time because such crystalline phases are reported to be formed after prolonged sorption time, *e.g.* 3 weeks. The DTA and TG curves are shown in Figures 3 and 4, respectively. Compared with the allophane sample, the phosphate-loaded samples show a slight change in the exothermic peaks, which correspond to crystallization. All the phosphate-loaded samples show the formation of cristobalite-type $AlPO_4$ after the DTA measurements, by contrast with the formation of mullite in the unloaded allophane. This difference may be correlated with the differences in the DTA exotherms. The TG curves (Figure 4) show similar weight losses irrespective of phosphate loading, with steep weight losses at 100ºC followed by gentler weight losses up to 500ºC. By

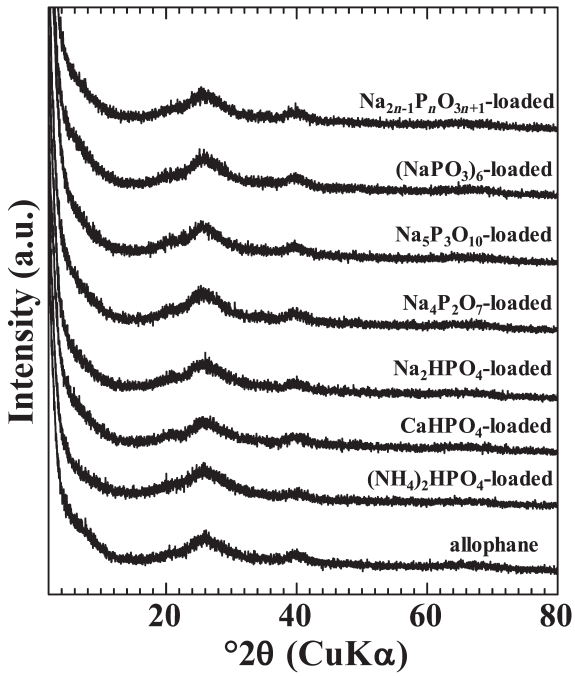

Figure 2. XRD patterns of allophane and phosphate-loaded allophanes.

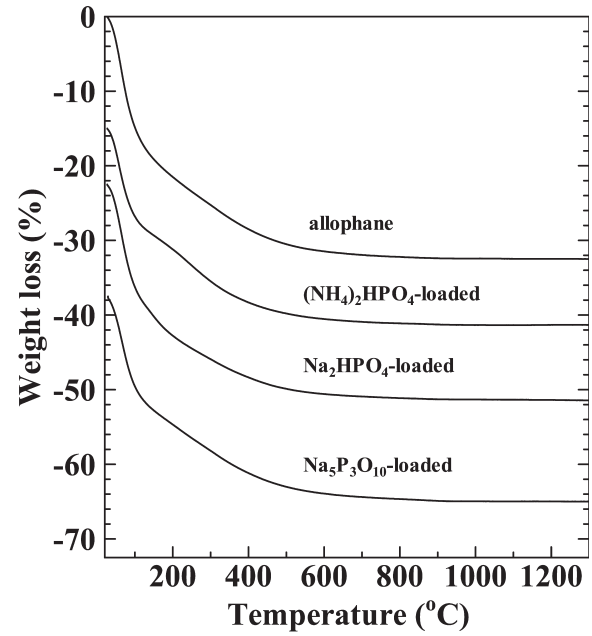

Figure 4. TG curves of allophane and phosphate-loaded allophanes.

contrast, the total weight losses differ clearly between the phosphate-loaded and unloaded samples. The weight losses of the phosphate-loaded allophane samples are: 26.3 wt.% ($(NH_4)_2HPO_4$-loaded sample), 29.0 wt.% (Na_2HPO_4-loaded sample) and 27.5 wt.% ($Na_5P_3O_{10}$-loaded sample). These values are smaller in the unloaded allophane (32.5 wt.%). The decreased weight losses of the phosphate-loaded samples show a good inverse linear correlation with the (Si+P)/Al ratio. Thus, the decreased weight loss can be explained by a decrease in the OH groups of the octahedral sheets caused by the loading of PO_4 tetrahedra on the surfaces of the octahedral sheets.

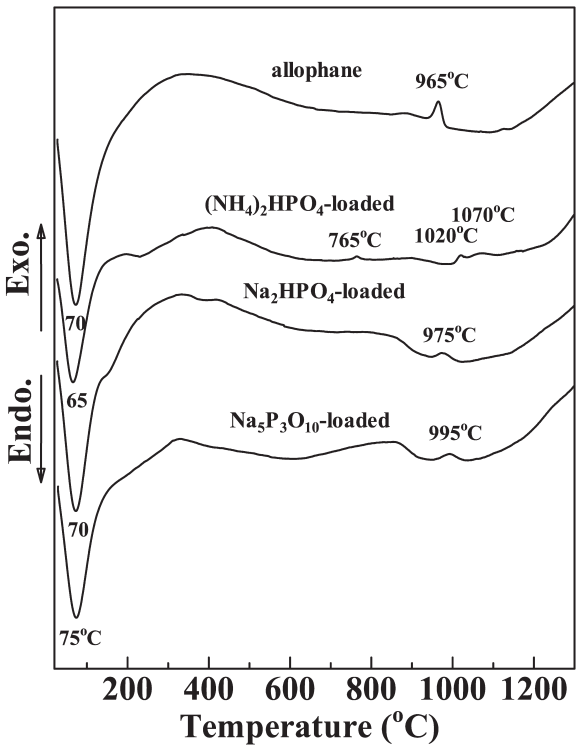

Figure 3. DTA curves of allophane and phosphate-loaded allophanes.

This phosphate loading was also examined by FTIR (Figure 5). The absorption bands of phosphate are known to occur in the wavelength range 900–1500 cm^{-1} (Nanzyo, 1995). However, the broad, strong absorption bands at ~1000 cm^{-1} in the $(NH_4)_2HPO_4$-loaded sample (b) are strongly affected by the absorption bands of the Si(Al)–O-stretching vibration of allophane (a); it is therefore necessary to use the difference spectrum method to determine the absorption bands of the loaded phosphate. The spectra (c–i) of Figure 5 are the difference spectra obtained by subtracting the spectrum of each phosphate-loaded sample from that of allophane. All the resulting spectra clearly show broad absorption bands at 1000–1200 cm^{-1}. The broadness of these bands is thought to reflect the overlap of the various phosphate species in the samples, most of which show strong absorption bands in this wavenumber range.

Characterization of loaded phosphate in the samples

The phosphate-loaded allophane was characterized by ^{29}Si, ^{27}Al and ^{31}P MAS NMR spectroscopy. As discussed above, the Si/Al ratio is decreased by orthophosphate loading but increased by polyphosphate

loading. The ^{29}Si and ^{27}Al MAS NMR spectra of unloaded allophane and samples loaded with $(NH_4)_2HPO_4$, Na_2HPO_4 and $Na_5P_3O_{10}$ are shown in Figures 6 and 7, respectively. The ^{27}Al NMR spectra are relatively unchanged by phosphate loading, all the samples showing a distinct peak at 5 ppm assigned to octahedral Al, with weak peaks due to tetrahedral Al occurring at 44 and 54−60 ppm. The appearance of the 44 ppm peak and decrease of the 54−60 ppm peak are observed in the orthophosphate-loaded samples, suggesting that orthophosphate loading may produce some change in the tetrahedral sites but polyphosphate loading does not. This difference is attributed to the difference in the amount of loaded PO_4 between the two series of samples. The solubility product of $AlPO_4$ (Stumm and Morgan, 1996), suggests the possible precipitation of $AlPO_4$ on the surface of the allophane. However, the ^{27}Al MAS NMR spectra do not support the formation of $AlPO_4$ even in an X-ray amorphous state because, as the Al atoms in $AlPO_4$ are in tetrahedral coordination, the tetrahedral NMR peak should increase after phosphate loading if $AlPO_4$ is formed.

By contrast with the ^{27}Al NMR spectra, the ^{29}Si NMR spectra of the phosphate-loaded samples show changes in the peak intensity ratio of the −78 and −89 ppm peaks ($R = I_{-89}/I_{-78}$). In this case, the former peak is assigned to a monomeric SiO_4 unit (Q^0) while the latter peak arises from polymerized tetrahedral units (Q^1−Q^3) (Lindner *et al.*, 1998) corresponding to the loaded PO_4 and to $Si(Al)O_4$ groups at the surface of the allophane particles. The peak intensity ratios R are increased by orthophosphate loading and increased further by polyphosphate loading.

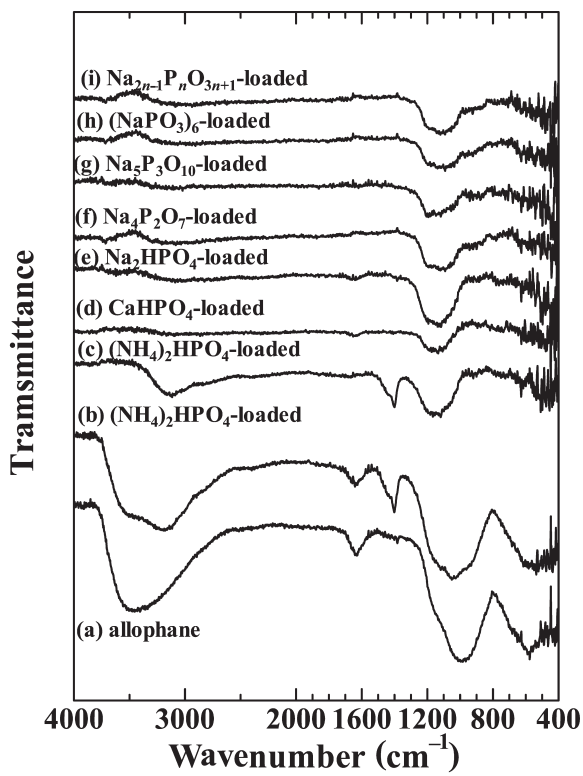

Figure 5. FTIR (a−b) and difference FTIR (c−i) spectra of allophane and phosphate-loaded allophanes.

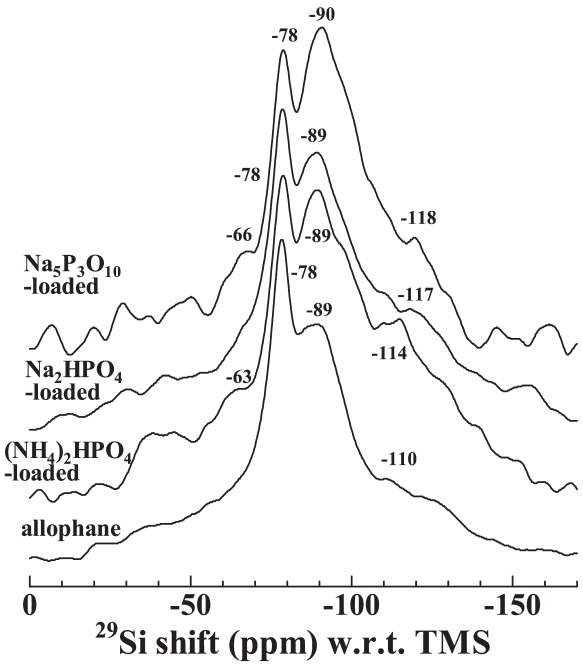

Figure 6. ^{29}Si MAS NMR spectra of allophane and phosphate-loaded allophanes.

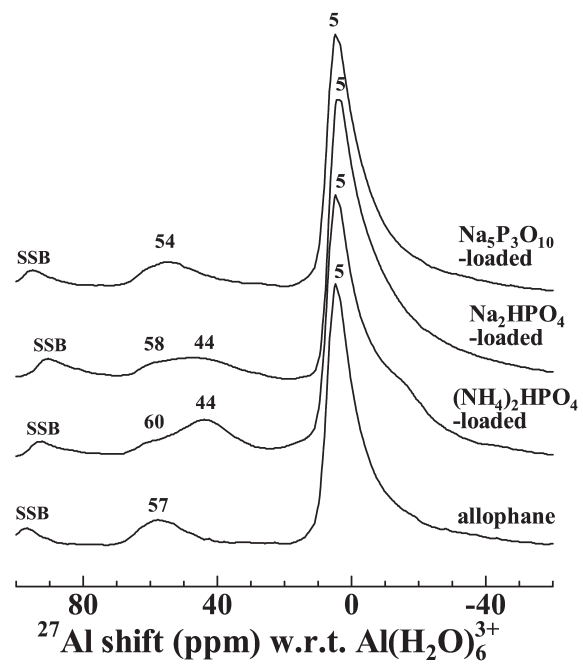

Figure 7. ^{27}Al MAS NMR spectra of allophane and phosphate-loaded allophanes. SSB: spinning side band.

The ^{31}P NMR spectra measured for the phosphate-loaded samples are shown in Figure 8. A relatively sharp peak is observed at ~−10 ppm in all the samples. The peak observed in the $Na_5P_3O_{10}$-loaded sample consists of two closely overlapping peaks at −8 and −12 ppm. Hayashi and Hayamizu (1989) reported the chemical shift values of various phosphates and found a relationship between the chemical shift values and the polymerized tetrahedral PO_4 structures similar to that found for Si NMR (MacKenzie and Smith, 2002). The chemical shifts range from 8 to 14 ppm in a Q^o unit (a monomeric structure), from −7 to 6 ppm in a Q^1 unit (a dimeric structure) and from −27 to −6 ppm in a Q^2 unit (a ring or chain structure). The chemical shift values decrease with increasing n values of the Q^n unit. Since the chemical shifts observed in the present phosphate-loaded samples range from −12 to −8 ppm (Figure 8), the PO_4 tetrahedra are therefore assigned to Q^2 units, suggesting that the phosphate loaded on allophane forms ring and/or chain structures associated with the $Si(Al)O_4$ tetrahedra present at the surface of the allophane particles.

The information on the allophane structure obtained in this study can be summarized as follows: (1) the Si/Al ratios of the samples show different trends with orthophosphate and polyphosphate loading, decreasing with orthophosphate loading but increasing with polyphosphate loading. By contrast, the (Si+P)/Al ratios fall in the narrow range 1.0−1.3. This implies an ~50−80% surface coverage of PO_4 and SiO_4 tetrahedra on the Al octahedral sheets of the allophane particles, assuming an imogolite-like structure (Si/Al ratio of 0.5) with the surface covered by excess tetrahedra. (2) The sample weight losses decrease with phosphate loading and correlate with the (Si+P)/Al ratios, suggesting that loading of the PO_4 tetrahedra occurs on the surface of the Al octahedral sheets of the allophane. (3) The loaded phosphates in the allophane are present in an X-ray amorphous state and no crystalline phosphate phases such as taranakite are detected in the XRD patterns. (4) The Al in the allophane is mainly in octahedral coordination but a very small amount of Al occurs in tetrahedral coordination. Phosphate loading produces little change in the Al coordination states. This suggests that no $AlPO_4$ is formed in the phosphate-loaded allophane samples even though such Al phosphate phase formation is possible on the basis of the solubility product. (5) Phosphate loading increases the amount of polymerized SiO_4 in the allophane because the loaded PO_4 bonds with $Si(Al)O_4$ tetrahedra forming polymerized tetrahedral structures on the surface of the Al octahedral sheets (6) The loaded phosphates show ^{31}P chemical shifts assigned to Q^2 units, suggesting the formation of ring and/or chain structures in conjunction with the $Si(Al)O_4$ tetrahedra mentioned above.

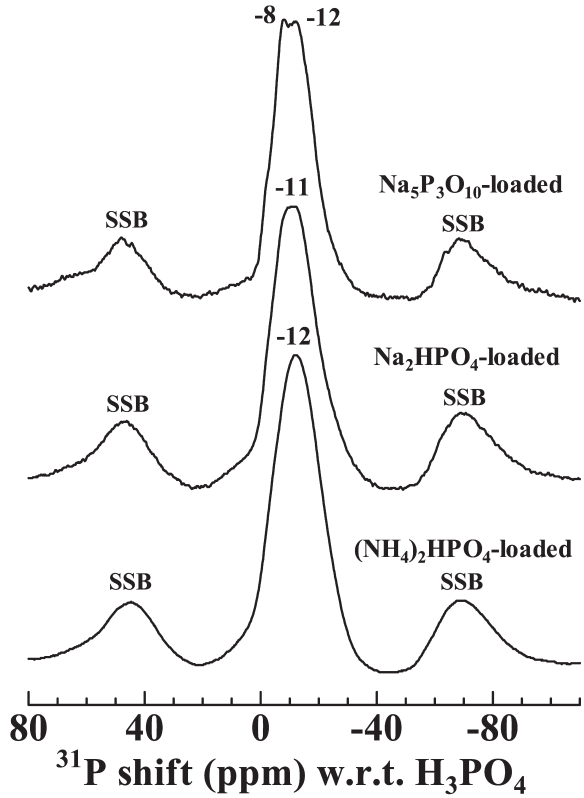

Figure 8. ^{31}P MAS NMR spectra of allophane and phosphate-loaded allophanes. SSB: spinning side band.

CONCLUSIONS

Phosphate loading on allophane of high Si/Al ratio (0.85) was performed using three orthophosphates and pyrophosphate, triphosphate, hexaphosphate and polyphosphate. The following results were obtained:

(1) Maximum phosphate sorption was achieved with $(NH_4)_2HPO_4$ loading. The isotherm was fitted better by the Langmuir equation than by the Freundlich equation and the maximum sorption capacity was 4.87 mmol/g. The sorption energy calculated from the Langmuir constant was −2.97 kJ/mol.

(2) The amount of loaded phosphate differed greatly depending on whether orthophosphates or polyphosphates were used. The chemical composition of the allophane assumed a lower Si/Al ratio with orthophosphate loading but the ratio became higher with polyphosphate loading.

(3) The weight loss of the samples decreased with phosphate loading, this effect becoming greater at higher (Si+P)/Al ratios. This result suggests that phosphate loading increases the surface coverage of the Al octahedral sheets of allophane by $Si(Al)O_4$ and PO_4 tetrahedra.

(4) The ^{29}Si MAS NMR spectra of allophane with and without phosphate loading show peaks at −78 (Q^o) and −89 ppm (Q^1−Q^3). The peak intensity ratio (I_{-89}/I_{-78}) increased with phosphate loading. The ^{27}Al MAS NMR

spectra show a distinct peak at 5 ppm corresponding to octahedral Al and a weak peak at 44–60 ppm corresponding to tetrahedral Al. Phosphate loading produced a slight shift of the tetrahedral Al peak but the octahedral Al peak was unchanged. The ^{31}P MAS NMR spectra show a peak at ~–10 ppm corresponding to a Q^2 unit (ring or chain structure), thought to consist of $Si(Al)O_4$ tetrahedra in conjunction with PO_4 tetrahedra.

REFERENCES

Clark, C.J. and McBride, M.B. (1985) Adsorption of Cu(II) by allophane as affected by phosphate. *Soil Science*, **139**, 412–421.

Elhadi, E.A., Matsue, N. and Henmi, T. (2000) Effect of molybdate adsorption on some surface properties of nano-ball allophane. *Clay Science*, **11**, 405–416.

Hayashi, S. and Hayamizu, K. (1989) High-resolution solid-state ^{31}P NMR of alkali phosphates. *Bulletin of the Chemical Society of Japan*, **62**, 3061–3068.

Johan, E., Matsue, N. and Henmi, T. (1997) Phosphate adsorption on nano-ball allophane and its molecular orbital analysis. *Clay Science*, **10**, 259–270.

Kitagawa, Y. (1971) The 'unit particle' of allophane. *American Mineralogist*, **56**, 465–475.

Lindner, G.-G., Nakazawa, H. and Hayashi, S. (1998) Hollow nanospheres, allophanes 'All-organic' synthesis and characterization. *Microporous and Mesoporous Materials*, **21**, 381–386.

MacKenzie, K.J.D. and Smith, M.E. (2002) *Multinuclear Solid-State NMR of Inorganic Materials*. Pergamon Materials Series, vol. **6**, Pergamon, Oxford, UK.

MacKenzie, K.J.D., Bowden, M.E. and Meinhold, R.H. (1991) The structure and thermal transformations of allophanes studied by ^{29}Si and ^{27}Al high resolution solid-state NMR. *Clays and Clay Minerals*, **39**, 337–346.

Naeem, A., Mustafa, S., Rehana, N., Dilara, B. and Murtaza, S. (2002) The sorption of divalent metal ions on $AlPO_4$. *Journal of Colloid and Interface Science*, **252**, 6–14.

Nanzyo, M. (1987) Formation of noncrystalline aluminum phosphate through phosphate sorption on allophanic Ando soils. *Communications of Soil Science and Plant Analysis*, **18**, 735–742.

Nanzyo, M. (1995) Reactions of phosphate with soil colloids. *Nendo-Kagaku*, **35**, 108–119.

Nartey, E., Matsue, N. and Henmi, T. (2001) Charge characteristics modification mechanisms of nano-ball allophane upon orthosilicic acid adsorption. *Clay Science*, **11**, 465–477.

Okada, K., Morikawa, H., Iwai, S., Ohira, Y. and Ossaka, J. (1975) A structure model of allophane. *Clay Science*, **4**, 291–303.

Padilla, G.N., Matsue, N. and Henmi, T. (2002a) Change in surface charge properties of nano-ball allophane as influenced by sulfate adsorption. *Clay Science*, **12**, 33–39.

Padilla, G.N., Matsue, N. and Henmi, T. (2002b) Adsorption of sulfate and nitrate on nano-ball allophane. *Clay Science*, **11**, 575–584.

Parfitt, R.L., Furkert, R.J. and Henmi, T. (1980) Identification and structure of two types of allophane from volcanic ash soils and tephra. *Clays and Clay Minerals*, **28**, 328–334.

Rajan, S.S.S. (1975) Mechanism of phosphate adsorption by allophane clays. *New Zealand Journal of Science*, **18**, 93–101.

Smith, J.P. and Brown, W.E. (1959) X-ray studies of aluminum and iron phosphates containing potassium or ammonium. *American Mineralogist*, **44**, 138–142.

Son, L.T., Matsue, N. and Henmi, T. (1998) Boron adsorption on allophane with nano-ball morphology. *Clay Science*, **10**, 315–325.

Stumm, W. and Morgan, J.J. (1996) *Aquatic Chemistry*, 3rd edition. John Wiley & Sons, Chichester, UK.

Tarasevich, Yu.I. and Klimova, G.M. (2001) Complex-forming adsorbents based on kaolinite, aluminium oxide and phosphates for the extraction and concentration of heavy metal ions from water solutions. *Applied Clay Science*, **19**, 95–101.

Wada, K. (1959) Reaction of phosphate with allophane and halloysite. *Soil Science*, **87**, 325–330.

Wada, K. (1979) Structural Formulas of Allophanes. *Proceedings of the 6th International Clay Conference, Oxford, 1978* (M.M. Mortland and V.C. Farmer, editors). Elsevier, Amsterdam, pp. 537–553.

(*Received 16 July 2004; revised 4 January 2005; Ms. 936; A.E. James E. Amonette*)